THE ROYAL SOCIETY

Critical amplitudes for pulse explosions with heat loss

By P. A. Blythe

Department of Mechanical Engineering and Mechanics, Lehigh University, Bethlehem, PA 18015, USA

Disturbances generated by the passage of pressure pulses through exothermic reacting mixtures are analysed for high frequency wave forms when the activation energy is large. Although wall heat loss can prevent ignition in the background state, heating within the pulse can give rise to local explosions. A determination of the critical pulse amplitude is made, and a response diagram is developed that permits a simple prediction of the final state at the end of the induction period.

Keywords: ignition; activation energy asymptotics; nonlinear convection; pulse explosions; fizzles; critical amplitudes

1. Introduction

Ignition calculations for vessel explosions at high activation energies (Semenov 1928; Kassoy 1977; Strehlow 1984) can be interpreted as the evaluation of a critical magnitude for the wall heat loss. For a subcritical case, in which the heat transfer rate is greater than the critical value, the spatially homogeneous response to departures from a low temperature state corresponds to a fizzle in which the temperature excursion is small. Spatially inhomogeneous dynamic changes associated with the propagation of pressure disturbances can, however, lead to explosive events even in situations where the background state is subcritical. This paper is concerned with the evolution of such disturbances and with the calculation of critical amplitudes that lead to thermal ignition.

Only one-dimensional unsteady disturbances are considered, and a suitable phenomenological model, based on Newton cooling, is used to describe heat loss to the surroundings. The applied signal is taken to be a small-amplitude, high-frequency pulse such that the time-scales for convective distortion, ignition, and background cooling are comparable. Analyses of this type, neglecting heat loss to the surroundings, have been given by Clarke (1978, 1979) and by Blythe (1978) for situations in which a dimensionless activation energy is large. Extensions to periodic signals have been given by Majda & Rosales (1987). Further results can be found in Almgren (1991), where particular emphasis is placed on shock formation. Some preliminary results including wall heat loss were discussed in Blythe (1978). In that paper, the heat loss term is dominated by the external (wall) temperature and does not reflect the more delicate balance that arises when the magnitude of the cooling is coupled to the gas temperature. It is the latter limit that is incorporated into the present investigation, which can be viewed as an extension of the classical analysis given by Semenov (1928).

Phil. Trans. R. Soc. Lond. A (1999) **357**, 3489–3502

Since, for all cases considered here, the background perturbation temperature T_∞ is a monotonic function of the time t, it is sometimes convenient to use T_∞ as a basic independent variable. In addition, the departure of the gas temperature from its background value, $\theta = T - T_\infty$, is a useful dependent variable. Appropriate conservation and rate laws are stated in § 2, and the background spatially homogeneous response is outlined in § 3. The large activation energy high-frequency limit is discussed in § 4, where the governing nonlinear evolution equation is obtained. In § 5 it is shown that solutions with subcritical heat loss can be conveniently classified in a (θ, T_∞) diagram. Use of this plane provides a simple means of predicting the limiting behaviour at the end of the induction domain. For a given heat transfer rate this outcome depends both on the initial pulse amplitude and on the relation of the background temperature to the wall temperature. Calculations of the critical dynamic (spatially inhomogeneous) amplitude as a function of the wall heat loss and of the initial gas temperature are presented.

In general, the applied signal is subject to amplitude dispersion, and shock formation is possible (Blythe 1978; Clarke 1978, 1979). Results for a particular input profile are obtained in § 6. It is noted there that situations can arise in which part of the pulse exceeds the critical dynamic amplitude and ultimately generates local ignition, whereas the remainder of the pulse collapses towards a fizzle state.

2. Conservation laws

For situations where the reactive and acoustic length-scales are comparable and much larger than relevant diffusive scales, conservation of mass and momentum is governed by the Euler equations

$$\partial_t \rho + \rho \frac{\partial u}{\partial x} = 0 \tag{2.1}$$

and

$$\rho \partial_t u + \frac{\partial p}{\partial x} = 0, \tag{2.2}$$

where the convective operator

$$\partial_t \equiv \frac{\partial}{\partial t} + u \frac{\partial}{\partial x}. \tag{2.3}$$

Here the pressure p and density ρ are made dimensionless with respect to their initial (starting) values $p'_{\rm s}$ and $\rho'_{\rm s}$ in the region $x > 0$, the velocity u is non-dimensionalized using $(p'_{\rm s}/\rho'_{\rm s})^{1/2}$, and primes denote dimensional quantities. Corresponding time- and distance-scales are introduced through

$$t' = t'_{\rm hi} t, \qquad x' = (p'_{\rm s}/\rho'_{\rm s})^{1/2} t'_{\rm hi} x, \tag{2.4}$$

where $t'_{\rm hi}$ is the spatially homogeneous ignition time associated with the initial state when heat loss to the surroundings is neglected (see § 3).

The caloric equation of state is assumed to have the general dimensionless form

$$e = e(p, \rho, y) \tag{2.5}$$

in which y is the reactant mass fraction; the specific internal energy e is also made dimensionless with respect to $p'_{\rm s}/\rho'_{\rm s}$. Similarly, the thermal equation of state is expressed as

$$T = T(p, \rho, y) \tag{2.6}$$

but the temperature T has been non-dimensionalized using the temperature $T'_{\rm w}$ of the external environment (see below).

Using (2.5) the energy equation can be formulated as

$$\partial_t p - a^2 \partial_t \rho + \rho\beta\partial_t y = -\rho Q(T; T_{\rm w}), \tag{2.7}$$

where $Q(T; T_{\rm w})$ is a phenomenological term representing heat lost to the surroundings, which are at a dimensionless temperature $T = T_{\rm w} = 1$. It is assumed that

$$Q(1; 1) = 0 \quad \text{with} \quad \left(\frac{{\rm d}Q}{{\rm d}T}\right)_{\rm w} > 0, \tag{2.8}$$

and the cooling mechanism is of the characteristic Newton type. Also in (2.7)

$$a = \left(\frac{p\rho^{-2} - \partial e/\partial\rho}{\partial e/\partial p}\right)^{1/2} \tag{2.9}$$

is the frozen isentropic sound speed, and

$$\beta = \frac{\partial e/\partial y}{\rho\partial e/\partial p} \tag{2.10}$$

is an effective heat release parameter. Since the formation energy

$$h_{\rm f} = \left.\frac{\partial h}{\partial y}\right|_{p,T}, \tag{2.11}$$

where $h(p, \rho, y)$ is the specific enthalpy, (2.10) can be written

$$\beta = \frac{\alpha_p a_T^2}{c_v}\left(h_{\rm f} + c_p\frac{\partial T}{\partial y}\right). \tag{2.12}$$

In (2.12) c_p and c_v are the frozen specific heats at constant pressure and constant volume, α_p is the frozen volumetric expansion coefficient, and a_T is the frozen isothermal sound speed. Note that

$$\alpha_p = -\frac{1}{\rho}\left.\frac{\partial\rho}{\partial T}\right|_{p,y}, \quad a_T^2 = \left.\frac{\partial p}{\partial\rho}\right|_{T,y} \quad \text{and} \quad \rho\alpha_p a_T^2 \equiv \left.\frac{\partial p}{\partial T}\right|_{\rho,y}. \tag{2.13}$$

Because of the non-dimensionalization adopted in (2.4), the appropriate form of the rate law for one-step Arrhenius kinetics is

$$\partial_t y = -\varepsilon N\Lambda(T) y \exp\{\varepsilon^{-1}(1 - T^{-1})\} \tag{2.14}$$

with

$$N = \left.\frac{c_v}{h_{\rm f} + (c_p - c_v)\partial T/\partial y}\right|_{\rm s}; \tag{2.15}$$

the suffix 's' denotes evaluation at the initial state. The assumption that the dimensionless inverse activation temperature

$$\varepsilon = \frac{T'_{\mathrm{w}}}{T'_{\mathrm{A}}} \ll 1 \tag{2.16}$$

is made throughout the analysis. ($T'_{\mathrm{A}} = E'_{\mathrm{A}}/R$, where E'_{A} is the activation energy and R is an appropriate gas constant.) Introduction of the factor N into the rate law is required by the definition of t'_{hi}. When there is no heat loss and the initial temperature and the wall temperature T_{w} are equal, i.e. $T_{\mathrm{s}} = T_{\mathrm{w}} = 1$, it follows that the dimensionless spatially homogeneous induction time $t_{\mathrm{hi}} \to 1$ as $\varepsilon \to 0$. Adoption of the specific exponential factor employed in (2.14) implies that, in general, the starting temperature $T_{\mathrm{s}} = 1 + O(\varepsilon)$. Note that the rate function Λ is such that

$$\Lambda_{\mathrm{s}} = 1. \tag{2.17}$$

It is convenient to put the conservation laws into characteristic form as

$$\partial_{\pm} p \pm \rho a \partial_{\pm} u = \rho(\Omega - Q), \tag{2.18}$$

where the characteristic derivatives

$$\partial_{\pm} \equiv \frac{\partial}{\partial t} + (u \pm a)\frac{\partial}{\partial x}. \tag{2.19}$$

Along particle paths

$$\partial_t p - a^2 \partial_t \rho = \rho(\Omega - Q). \tag{2.20}$$

In (2.18) and (2.19)

$$\Omega = \varepsilon N \beta(p, \rho, y) \Lambda(T) y \exp\{\varepsilon^{-1}(1 - T^{-1})\}, \tag{2.21}$$

and the rate law (2.14) can be written

$$\partial_t y = -\beta^{-1} \Omega(p, \rho, y). \tag{2.22}$$

These equations are to be solved subject to the initial conditions

$$p = \rho = y = 1, \quad T = T_{\mathrm{s}}, \quad \text{and } u = 0 \text{ at } t = 0,\ x > 0. \tag{2.23}$$

Only high-frequency, small-amplitude pulses are considered in this paper. The signals are generated by piston motions of the form $x = \varepsilon^2 x_p(t/\varepsilon)$ or

$$u = \varepsilon u_p(t/\varepsilon) \quad \text{on } x = \varepsilon^2 x_p. \tag{2.24}$$

Blythe (1978), Clarke (1978, 1979), Majda & Rosales (1987) and Almgren (1991) have previously studied this distinguished limit in which the signal amplitude and the signal time-scale are comparable with the inverse activation temperature ε. The adoption of (2.24) leads to a non-trivial far-field structure (see § 4), where amplitude dispersion, chemistry, heat loss, and background disturbances have balancing contributions. Moreover, if the pulse width is $\varepsilon \bar{t}_p$, the shape function satisfies

$$u_p(0) = u_p(\bar{t}_p) = 0 \tag{2.25}$$

so that, before shock formation, the leading edge and the tail of the signal correspond to acceleration fronts.

3. Background state

Before the arrival of the applied signal, a spatially homogeneous reaction takes place in the gas. Inspection of the rate law and energy equation indicates that finite changes in the reaction rate occur for $\Delta T = O(\varepsilon)$ and $\Delta y = O(\varepsilon)$. Suitable expansions for this induction phase are (Kassoy 1977)

$$\Psi(t;\varepsilon) = \Psi_{\rm s} + \varepsilon\Psi_{1\infty}(t)\ldots, \tag{3.1}$$

where Ψ represents p, T, or y. In addition,

$$u = u_{\rm s} = 0, \qquad \rho = \rho_{\rm s} = 1. \tag{3.2}$$

Consistent with this expansion, and with the distinguished limit outlined in § 2, it is necessary to take

$$T_{\rm s} = 1 + \varepsilon T_{1{\rm s}}. \tag{3.3}$$

From (2.18)–(2.22), it is not difficult to establish that

$$\frac{{\rm d}T_\infty}{{\rm d}t} = \exp(T_\infty) - qT_\infty \tag{3.4}$$

and

$$\frac{{\rm d}y_\infty}{{\rm d}t} = -N\exp T_\infty. \tag{3.5}$$

For convenience, in (3.4) and (3.5), the subscript '1' has been omitted from the perturbation terms, and

$$q = \left.\frac{({\rm d}Q/{\rm d}T)}{\alpha_p a_T^2}\right|_{\rm s} > 0. \tag{3.6}$$

Since

$$T_\infty(0) = T_{\rm s} \quad \text{and} \quad y_\infty(0) = 0, \tag{3.7}$$

where the subscript '1' has again been omitted,

$$t = \int_{T_{\rm s}}^{T_\infty} \frac{{\rm d}s}{{\rm e}^s - qs}, \tag{3.8}$$

$$y_\infty = -N\int_{T_{\rm s}}^{T_\infty} \frac{{\rm e}^s}{{\rm e}^s - qs}\,{\rm d}s, \tag{3.9}$$

and

$$p_\infty = (\rho\alpha_p a_T^2)_{\rm s}[T_\infty - T_{\rm s} - (\partial T/\partial y)_{\rm s} y_\infty]. \tag{3.10}$$

When $q = 0$ and $T_{\rm s} = 0$,

$$T_\infty = -\ln(1-t) \tag{3.11}$$

and, as noted in § 2, $t = t_{\rm hi} = 1$ at ignition. For $T_{\rm s} > 0$ the gas temperature is initially hotter than that of the surroundings; $T_{\rm s} < 0$ corresponds to a lower initial gas temperature.

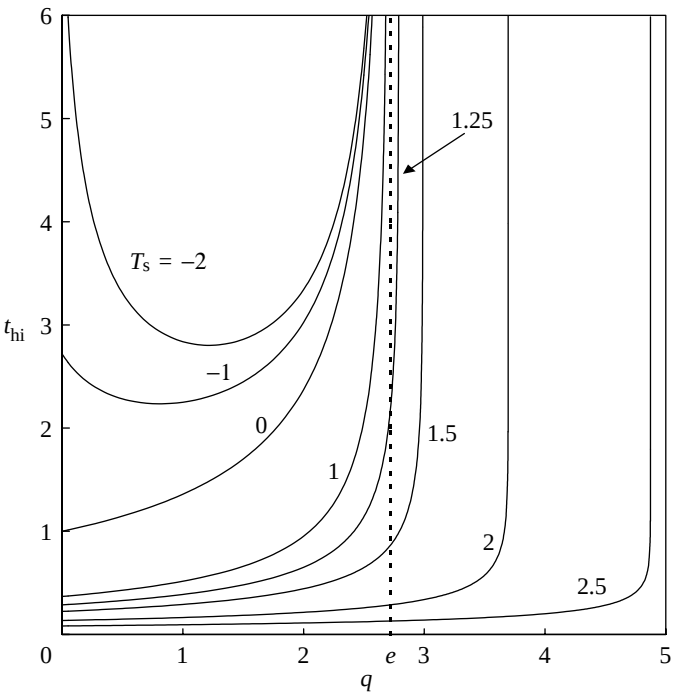

Figure 1. Spatially homogeneous ignition times as a function of the wall heat loss for various initial gas temperatures.

If the wall heat transfer rate is sufficiently low, specifically

$$q < q_{\mathrm{crit}} = e, \tag{3.12}$$

ignition will always occur at a time given by

$$t = t_{\mathrm{hi}}(q; T_{\mathrm{s}}) = \int_{T_{\mathrm{s}}}^{\infty} \frac{\mathrm{d}s}{\mathrm{e}^s - qs}. \tag{3.13}$$

For $q > q_{\mathrm{crit}}$ there are two roots $(T_{\mathrm{h1}}, T_{\mathrm{h2}})$ of $\mathrm{e}^T = qT$ with

$$T_{\mathrm{h1}} < 1 < T_{\mathrm{h2}}. \tag{3.14}$$

If $T_{\mathrm{s}} \equiv T_\infty(0) < T_{\mathrm{h2}}$, then all solutions correspond to a fizzle such that

$$T_\infty \to T_{\mathrm{h1}} \quad \text{as} \quad t \to \infty. \tag{3.15}$$

When $T_{\mathrm{s}} > T_{\mathrm{h2}}$ ignition occurs irrespective of the magnitude of q, and the homogeneous ignition time is still defined by (3.13). The function $t_{\mathrm{hi}}(q; T_{\mathrm{s}})$ is displayed in figure 1.

From the above discussion it is apparent that if $T_{\mathrm{s}} < 1 < T_{\mathrm{h2}}$, then t_{hi} becomes unbounded as $q \to e-$. Again $e \equiv q_{\mathrm{crit}}$. In particular, it can be established that

$$t_{\mathrm{hi}} \sim \pi(2/e)^{1/2}(e-q)^{-1/2} \quad \text{as} \quad q \to e- . \tag{3.16}$$

Near $T_{\mathrm{s}} = 1$, (3.16) can be extended to give

$$t_{\mathrm{hi}} \sim (2/e)^{1/2}((\pi/2) + \arctan\phi)(e-q)^{-1/2}, \tag{3.17}$$

where

$$\phi = \left(\frac{e}{2(e-q)}\right)^{1/2}(T_{\rm s}-1). \tag{3.18}$$

Consequently, at $T_{\rm s}=1$

$$t_{\rm hi} \sim \frac{\pi}{\sqrt{2e}}(e-q)^{-1/2} \tag{3.19}$$

and the growth rate is one-half of that for $1-T_{\rm s}=O(1)$ (see (3.17)).

When $T_{\rm s}>1$ the algebraic growth associated with (3.17) is replaced by a logarithmic behaviour. Specifically, on $q=q_{\rm crit}$ with $T_{\rm s}-1=o(1)$, all solutions have a finite ignition time given by

$$t_{\rm hi} = \frac{2}{e(T_{\rm s}-1)} + \frac{2}{3e}\ln(T_{\rm s}-1) + O(1). \tag{3.20}$$

For any given $T_{\rm s}>1$ the solution corresponds to a thermal explosion provided that

$$q < q_{\max} = T_{\rm s}^{-1}\exp T_{\rm s}. \tag{3.21}$$

Note that when $e<q<q_{\max}$

$$T_{\rm h2}^{-1}\exp T_{\rm h2} < T_{\rm s}^{-1}\exp T_{\rm s}. \tag{3.22}$$

As noted earlier, since $T_{\rm h2}>1$, explosions occur for $q>e$ when

$$T_{\rm s} > T_{\rm h2}, \tag{3.23}$$

and as $q\to q_{\max}-$ it can be established that

$$t_{\rm hi} \sim -\frac{T_{\rm s}}{T_{\rm s}-1}\ln(q_{\max}-q) + O(1). \tag{3.24}$$

The results (3.17)–(3.24) are reflected in the data displayed in figure 1.

4. Far-field structure

When t and x are $O(\varepsilon)$ the near-field structure for high-frequency signals of the form (2.24) is governed by

$$p-1 = a_{\rm s}^2(\rho-1) = a_{\rm s}u = \varepsilon a_{\rm s}u_p(\xi_1), \tag{4.1}$$

where

$$\xi_1 = \varepsilon^{-1}(t-a_{\rm s}^{-1}x), \tag{4.2}$$

and the subscript 's' again denotes evaluation at the initial upstream state. Also

$$T-T_{\rm s} = k_\rho^{-1}(\rho-1) \tag{4.3}$$

with

$$k_\rho = \left(\frac{\partial\rho}{\partial T}\bigg|_{\sigma,y}\right)_{\rm s} = \left(\frac{\rho\alpha_p}{\gamma-1}\right)_{\rm s}. \tag{4.4}$$

In (4.4) σ is the specific entropy and γ is the frozen specific heat ratio; the volumetric expansion coefficient α_p was defined in (2.13). It follows that within this region

$$y - 1 = O(\varepsilon^2). \tag{4.5}$$

Over a time-scale $t = O(\varepsilon)$, the upstream perturbations p_∞, T_∞, etc., are also $O(\varepsilon^2)$. (For ease of writing, the subscript '1' is again omitted from the perturbation terms.) Clearly, the leading-order structure in the near-field corresponds to the standard linearized frozen acoustic signal. Consideration of higher-order terms, however, indicates that secular behaviour can develop over a time-scale comparable with the local induction time. In this far-field region $t = O(1)$ and it is appropriate to introduce a front variable

$$\bar{\xi} = \frac{x_\infty(t;\varepsilon) - x}{\varepsilon} = O(1), \tag{4.6}$$

where

$$\frac{\mathrm{d}x_\infty}{\mathrm{d}t} = a_\infty(t;\varepsilon) = a_\mathrm{s} + \varepsilon a_{1\infty}(t) + \ldots. \tag{4.7}$$

Matching with the near-field behaviour, and with the background solution, implies that the local solution has the form

$$\psi(t, x;\varepsilon) = \psi_\mathrm{s} + \varepsilon\psi_1(t, \bar{\xi}) + \ldots. \tag{4.8}$$

Here ψ represents T, p, ρ, u or y. Note that

$$p_\mathrm{s} = 1, \quad \rho_\mathrm{s} = 1, \quad y_\mathrm{s} = 1, \quad u_\mathrm{s} = 0 \quad \text{and} \quad T_\mathrm{s} = 1 + \varepsilon T_{1\mathrm{s}}. \tag{4.9}$$

As in the near field, the dependent variables relative to their background state satisfy the linearized acoustic relations

$$p_1 - p_{1\infty}(t) = a_\mathrm{s}^2\rho_1 = a_\mathrm{s}u_1 \tag{4.10}$$

with

$$T_1 - T_{1\infty}(t) \equiv \theta(t, \bar{\xi}) = k_\rho^{-1}\rho_1 \quad \text{and} \quad a_1 - a_{1\infty}(t) = k_a\theta, \tag{4.11}$$

where, for $a = a(p, \rho, y)$,

$$k_a = \left(\frac{\partial a}{\partial T}\bigg|_{\sigma,y}\right)_\mathrm{s} = k_\rho\left(\frac{\partial a}{\partial \rho} + a^2\frac{\partial a}{\partial p}\right)_\mathrm{s}. \tag{4.12}$$

Substitution of these results into the first of the characteristic relations (2.18) yields the nonlinear evolution equation

$$\frac{\partial\theta}{\partial t} - \theta\frac{\partial\theta}{\partial\xi} = m(n\mathrm{e}^{T_{1\infty}}(\mathrm{e}^\theta - 1) - q\theta), \tag{4.13}$$

where $\bar{\xi} = b\xi$ and

$$b = \left(\frac{1}{\rho}\frac{\partial}{\partial T}(\rho a)\bigg|_{\sigma,y}\right)_\mathrm{s}, \quad m = \left(\frac{\gamma - 1}{2\gamma}\right)_\mathrm{s} \quad \text{and} \quad n = \left(\frac{h_\mathrm{f} + c_p(\partial T/\partial y)}{h_\mathrm{f} + (c_p - c_v)(\partial T/\partial y)}\right)_\mathrm{s}. \tag{4.14}$$

Introduction of the characteristic paths

$$\left.\frac{\partial \xi}{\partial t}\right|_{\alpha} = -\theta \quad \text{with } \xi = \alpha \text{ on } t = 0 \tag{4.15}$$

enables (4.13) to be written

$$\left.\frac{\partial \theta}{\partial t}\right|_{\alpha} = m(n\mathrm{e}^{T_{1\infty}}(\mathrm{e}^{\theta} - 1) - q\theta). \tag{4.16}$$

The solution of (4.16) must satisfy the near-field matching condition

$$\theta = \theta_p(\alpha) \equiv a_{\mathrm{s}}^{-1} k_{\rho}^{-1} u_p(a_{\mathrm{s}}^{-1} b\alpha) \quad \text{on } t = 0. \tag{4.17}$$

5. The (θ, T_{∞})-plane

Since (4.16) and (3.4) are autonomous, the solution along any characteristic path is governed by

$$\left.\frac{\partial \theta}{\partial T_{\infty}}\right|_{\alpha} = m\frac{n\mathrm{e}^{T_{\infty}}(\mathrm{e}^{\theta} - 1) - q\theta}{\mathrm{e}^{T_{\infty}} - qT_{\infty}}. \tag{5.1}$$

The case where the background state is subcritical, with

$$q > q_{\mathrm{crit}} = e, \tag{5.2}$$

is of considerable interest. As noted in § 3, provided that $T_{\mathrm{s}} < T_{\mathrm{h2}}$ the restriction (5.2) always leads to a fizzle in the upstream region. Under these circumstances, determination of the critical amplitude $\theta_p(\alpha)$ that triggers ignition is definitely of significance.

The phase equation (5.1), subject to (5.2), has four critical points:

$$\text{(i)} \quad (T_{\mathrm{h1}}, \theta_1); \qquad \text{(ii)} \quad (T_{\mathrm{h1}}, 0); \qquad \text{(iii)} \quad (T_{\mathrm{h2}}, \theta_2); \qquad \text{(iv)} \quad (T_{\mathrm{h2}}, 0), \tag{5.3}$$

where θ_i is the root of

$$\frac{\theta}{\exp\theta - 1} = nT_{\mathrm{h}i}. \tag{5.4}$$

In the special case when the dimensionless formation energy $h_{\mathrm{f}} \gg 1$, then

$$n \approx 1 \tag{5.5}$$

and (5.4) has solutions

$$\theta_1 = -\theta_2 = T_{\mathrm{h2}} - T_{\mathrm{h1}}. \tag{5.6}$$

Typical integral curves for the case (5.5) are shown schematically in figure 2. Points (i) and (iii) correspond to saddles, whereas (ii) is a stable node and (iv) is an unstable node. All solutions for which the initial state $T_{\mathrm{s}} = T_{\infty}(0) < T_{\mathrm{h2}}$ will correspond to explosions ($\theta \to \infty$ at a finite time) provided that

$$\theta_p > \theta_{\mathrm{sa}}(T_{\infty}), \tag{5.7}$$

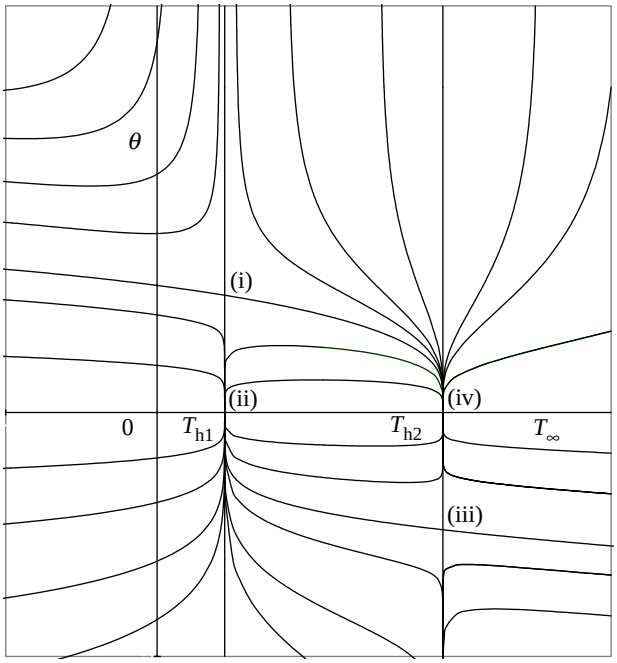

Figure 2. Typical integral curves in the (θ, T_∞)-plane.

where $\theta_{sa}(T_\infty)$ is the saddle curve passing through point (i). Solutions for which

$$\theta_p < \theta_{sa}(T_s) \quad \text{and} \quad T_s < T_{h1} \tag{5.8}$$

lead to a fizzle with $T \to T_{h1}$ as $t \to \infty$. If $T_s > T_{h2}$, all solutions correspond to thermal explosions and, when $\theta_p > 0$, ignition occurs within the pulse. If $\theta_p < 0$, it can be established that

$$T \sim (1 - mn)T_\infty \quad \text{as} \quad T_\infty \to \infty. \tag{5.9}$$

When the effective heat release β and the formation energy h_f are both positive it can be shown that, irrespective of the sign of $\partial T/\partial y$,

$$1 > mn > 0. \tag{5.10}$$

Consequently, for expansions ($\theta_p < 0$) the temperature within the pulse is lower than that in the upstream region and a thermal explosion will first occur outside the pulse.

The phase diagram in figure 2 is appropriate for

$$\text{(a)} \quad nT_{h2} > 1 > nT_{h1}. \tag{5.11}$$

Phase diagrams for the additional cases

$$\text{(b)} \quad 1 > nT_{h2} > nT_{h1} \quad \text{and} \quad \text{(c)} \quad 1 < nT_{h1} < nT_{h2} \tag{5.12}$$

are easily obtained. Although the classification of the individual critical points can change, the phase plots are topologically equivalent and the overall behaviour is summarized in table 1.

For case (c) it should be noted that $\theta_{sa} = 0$. Examples of $\theta_{sa}(T_\infty)$ are shown in figure 3 for various q with $n = 1$.

Table 1. *Summary of system responses for $q > e$*

initial state	pulse amplitude	result
$T_\infty(0) < T_{\mathrm{h}2}$	$\theta_p > \theta_{\mathrm{s}}$	pulse explosion
$T_\infty(0) < T_{\mathrm{h}2}$	$\theta_p < \theta_{\mathrm{s}}$	fizzle
$T_\infty(0) > T_{\mathrm{h}2}$	$\theta_p > 0$	pulse explosion
$T_\infty(0) > T_{\mathrm{h}2}$	$\theta_p < 0$	background explosion

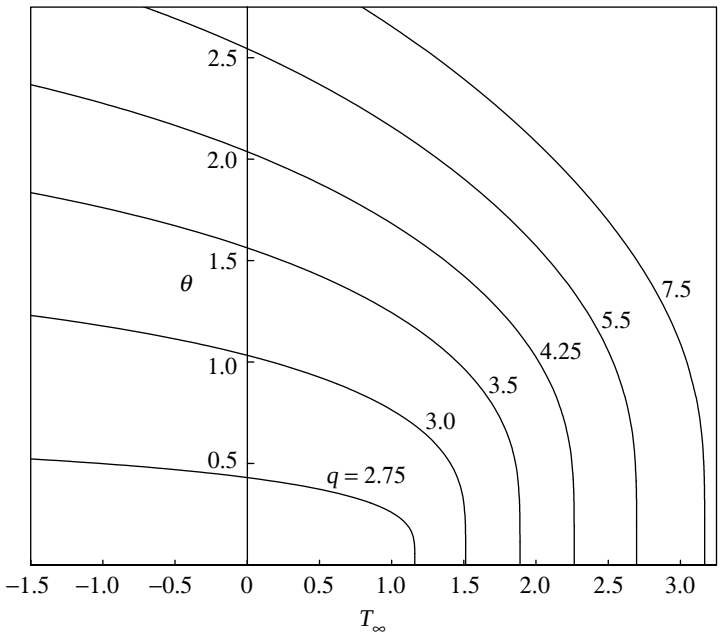

Figure 3. Critical amplitudes.

6. Pulse evolution

For ease of discussion it is assumed in this section that $n = 1$. The solution in the (θ, T_∞)-plane enables

$$\theta = \theta(t, \alpha; T_{\mathrm{s}}) \tag{6.1}$$

to be obtained for a given input signal $\theta_p(\alpha)$ and for prescribed values of q and γ. As noted in § 5, for $T_{\mathrm{s}} < T_{\mathrm{h}2}$ and $q > e$, amplification will occur only in those parts of the signal that satisfy

$$\theta_p > \theta_{\mathrm{crit}}(q; T_{\mathrm{s}}, \gamma) \equiv \theta_{\mathrm{sa}}. \tag{6.2}$$

If the starting amplitude is below θ_{crit}, the solution at fixed α corresponds to a fizzle with $\theta \to 0$ as $t \to \infty$.

Typical profiles are shown in figure 4 as a function of the characteristic coordinate α for various times t; the input shape

$$\theta_p = 3 \sin \alpha, \qquad 0 \leqslant \alpha \leqslant \pi, \tag{6.3}$$

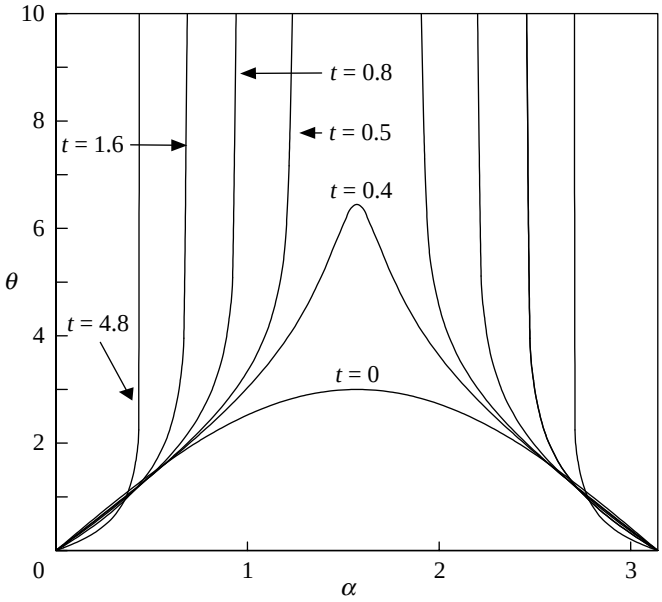

Figure 4. Evolution of the α-plane.

is symmetrical about $\alpha = \pi/2$. In figure 4, $q = 3$, $\gamma = 7/5$. For simplicity, it is assumed that the gas and environment temperatures are initially equal, so that $T_{\mathrm{s}} = 0$. For this example it can be established that

$$\theta_{\mathrm{crit}} \approx 0.8931 \tag{6.4}$$

and the minimum ignition time

$$t_{\mathrm{min}} \approx 0.4089. \tag{6.5}$$

The ignition event associated with (6.5) is clearly visible in figure 4, as is the limiting behaviour characterized by (6.2).

If $\theta_p(\alpha)$ is symmetric then, at a given time t, so is $\theta(t, \alpha)$. In the physical (t, ξ)-plane, however, the pulse shape is subject to amplitude dispersion. At constant α, with $\theta(t, \alpha)$ calculated from (5.1) and (4.17), it follows from (4.15) that

$$\xi = \alpha - \int_0^t \theta(s, \alpha)\,\mathrm{d}s = \alpha - \int_0^{T_\infty} \frac{\theta(t(v), \alpha)}{\mathrm{e}^v - qv}\,\mathrm{d}v, \tag{6.6}$$

where $t(T_\infty)$ is defined by (3.8). Spatio-temporal development of the wave profile is shown in figure 5 for the particular case specified in (6.3). From the figure it is apparent that the solutions are not single valued for all t. In general, this lack of uniqueness arises when

$$\left.\frac{\partial \xi}{\partial \alpha}\right|_t = 0. \tag{6.7}$$

For the pulse (6.3) this first occurs at a time

$$t_{\mathrm{sf}} \approx 0.3478 \quad \text{with} \quad \xi \approx 1.48 \times 10^{-4}. \tag{6.8}$$

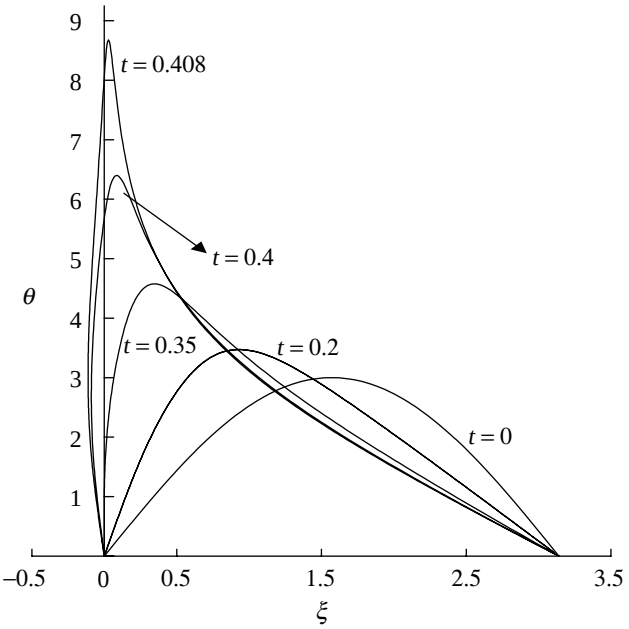

Figure 5. Sine pulse evolution.

Subsequent to t_{sf}, a shock wave develops. A discussion of shock paths is not given in this paper, but an example for the case when $q = 0$ can be found in Clarke (1979). Nevertheless, if ignition occurs along a given characteristic on which $\theta_p > 0$ and $\mathrm{d}\theta_p/\mathrm{d}\alpha > 0$ it follows from (3.4), (5.1), and (6.6) that shock formation (lack of uniqueness) must precede this event. As noted by Clarke (1979), on a path for which $\mathrm{d}\theta_p/\mathrm{d}\alpha \equiv 0$, then $\partial\xi/\partial\alpha \equiv 1$, and ignition apparently occurs before local shock formation. Consideration of the limit $\mathrm{d}\theta_p/\mathrm{d}\alpha \to 0+$ indicates, however, that ignition and local shock formation coincide as the turning point is approached. Further analysis of this region could yield some useful information concerning the possible birth of a strong reaction wave or fast flame.

An earlier version of this paper was presented at the symposium on Combustion Science at the End of the Millennium held at the University of Cambridge, April 1997. The work was completed while the author was visiting the Department of Applied Mathematics and Theoretical Physics at the University of Cambridge and its hospitality was much appreciated; he is also grateful to the EPSRC for support during this period.

References

Almgren, R. F. 1991 High frequency acoustic waves in a reacting gas. *SIAM J. Appl. Math.* **51**, 351–373.

Blythe, P. A. 1978 Wave propagation and ignition in a combustible mixture. In *17th Int. Symp. on Combustion*, pp. 909–916. Pittsburgh: The Combustion Institute.

Clarke, J. F. 1978 Small amplitude gas dynamic disturbances in an exploding atmosphere. *J. Fluid Mech.* **89**, 343–355.

Clarke, J. F. 1979 On the evolution of compression pulses in an exploding atmosphere: initial behaviour. *J. Fluid Mech.* **94**, 195–208.

Kassoy, D. R. 1977 The supercritical spatially homogeneous thermal explosion: initiation to completion. *Q. J. Mech. Appl. Math.* **30**, 71–89.

Majda, A. J. & Rosales, R. R. 1987 Nonlinear mean field–high frequency wave interactions in the induction zone. *SIAM J. Appl. Math.* **47**, 1017–1039.

Semenov, N. N. 1928 Zur Theorie des Verbrennungsprozesses. *Z. Phys.* **48**, 571–582.

Strehlow, R. A. 1984 *Combustion fundamentals*. McGraw-Hill.